NOTES AND CORRESPONDENCE

The AVHRR Channel 3 Cloud Top Reflectivity of Convective Storms

MARTIN SETVÁK

Czech Hydrometeorological Institute, Prague, Czechoslovakia

CHARLES A. DOSWELL III

NOAA/Environmental Research Laboratories, National Severe Storms Laboratory, Norman, Oklahoma

4 May 1990 and 1 October 1990

1. Introduction

The advanced very high resolution radiometer (AVHRR) aboard the NOAA polar orbiting satellites produces high-resolution (nominal resolution at nadir of 1.1 km) images of clouds in the 3.55–3.93 μm band, the so-called channel 3 window. In this channel, nominally centered at 3.7 μm, reflected and emitted radiation comprise roughly equal fractions of the received radiance during the daylight hours. Which of these two components is dominant depends on several parameters, including the temperature of the emitter, the solar zenith angle, and the reflectivity of objects (albedos) within this spectral window. The character of the reflectivity in the channel 3 data is quite different from that in the visible (channel 1, 0.58–0.68 μm) and near infrared (NIR—channel 2, 0.725–1.1 μm) spectral windows; for instance, ice behaves in the channel 3 window very nearly like a blackbody (i.e., an albedo near zero).

A method for computation of the channel 3 reflectivity has been developed at the Czech Hydrometeorological Institute (CHMI) at Prague, Czechoslovakia. Some quite interesting images are obtained when applying this technique to situations involving deep convective storms. Occasional storms exhibit an increased channel 3 cloud top reflectivity (hereafter referred to as CH3 CTR) that appears to be related to the microphysical properties of the convective cloud tops. In turn, there appears to be some relation between such cloud top signatures and storm severity, especially with regard to hail, although such a relationship can only be considered tentative as of this writing.

2. Computation of channel 3 reflectivity

If ϵ_3 denotes the channel 3 emissivity and α_3 is the channel 3 reflectivity, the total radiance (N_3) measured by the satellite during the daylight hours can be expressed as

$$N_3 = N_{3(ref)} + \epsilon_3 N_3(T), \tag{1}$$

where $N_{3(ref)}$ stands for the reflected component and $N_3(T)$ is the emitted component for a blackbody at temperature T(K), which is found by computing the Planck function appropriate for channel 3 (see Lauritson et al. 1979 or d'Entremont and Kleespies 1988). The reflected component in (1) can be determined from

$$N_{3(ref)} = \alpha_3 N_3(T_s)(R/r)^2 \cos\xi, \tag{2}$$

where T_s is the blackbody temperature of the solar photosphere (5800 K), R is the radius of the sun, r is the radius of the earth's orbit, and ξ is the solar zenith angle. For convenience, let

$$S_3(r, \xi) \equiv N_3(T_s)(R/r)^2 \cos\xi, \tag{3}$$

where S_3 is the solar flux at the top of the atmosphere, so that (1) can be rewritten using (2) and (3) as

$$N_3 = \alpha_3 S_3(r, \xi) + \epsilon_3 N_3(T). \tag{4}$$

Observe that this assumes the independence of α_3 and ϵ_3 with respect to wavelength of the radiation within the window of channel 3. For sufficiently dense clouds, it is reasonable to assume a zero transmissivity, so Kirchoff's Law reduces to

$$\alpha_3 + \epsilon_3 = 1. \tag{5}$$

From (4) and (5), it is easy to derive the following relations for computation of the AVHRR channel 3 emissivity and reflectivity:

$$\epsilon_3 = \frac{N_3 - S_3(r, \xi)}{N_3(T) - S_3(r, \xi)}, \tag{6}$$

$$\alpha_3 = \frac{N_3 - N_3(T)}{S_3(r, \xi) - N_3(T)}. \tag{7}$$

Corresponding author address: Dr. Charles A. Doswell III, National Severe Storms Laboratory, 1313 Halley Circle, Norman, OK 73069.

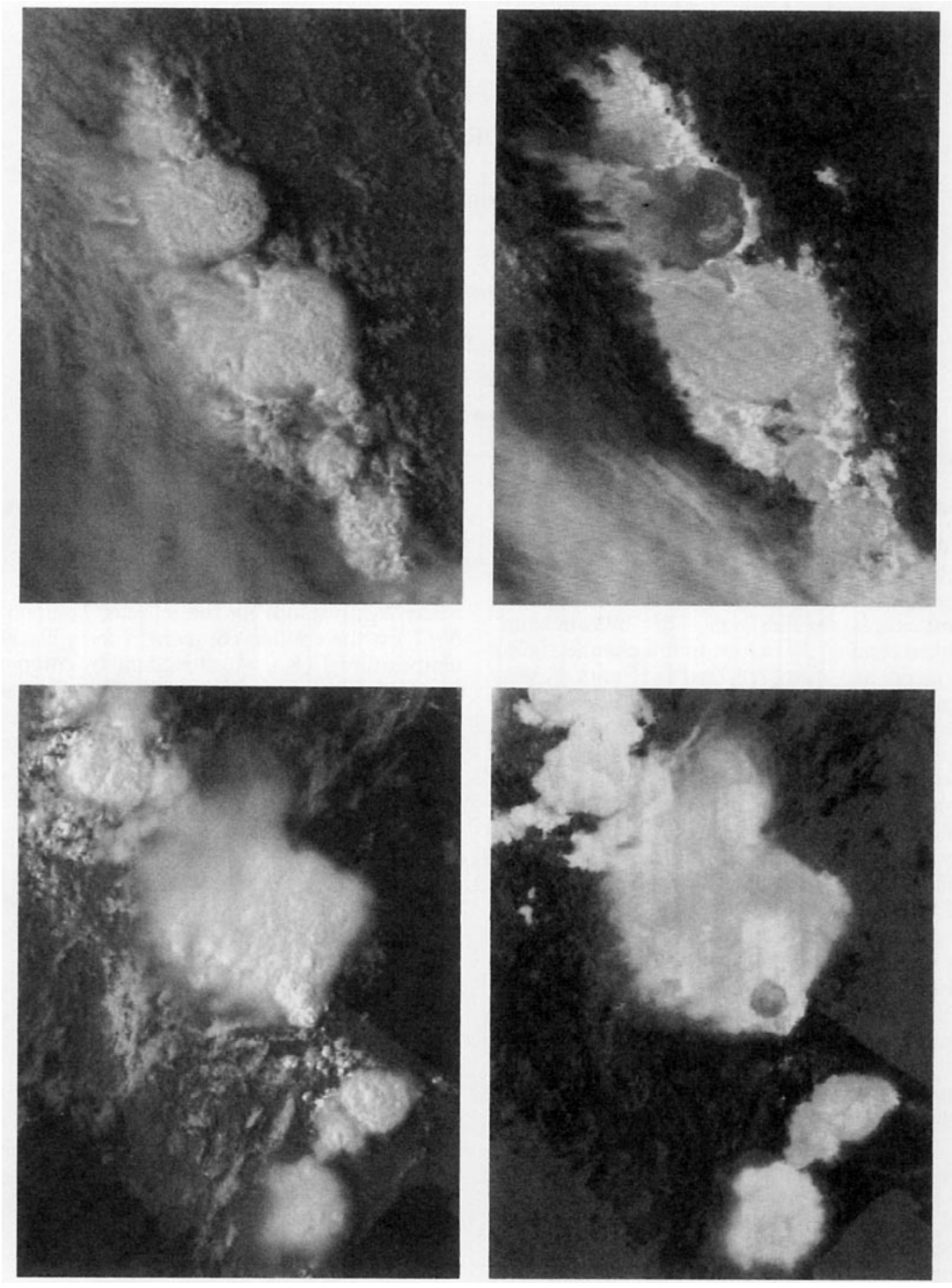

FIG. 1. Examples of storms exhibiting "convective cell' type of signature in channel 3 cloud top reflectivity. On the left of each figure is the channel 2 (visible image) and on the right is the channel 3 image, as discussed in the text, each with north at the top. The first example (a) shows storms over Germany and Czechoslovakia on 4 June 1984 (1335 UTC, NOAA-7), the second (b) shows storms over central Italy on 9 July 1987 (1355 UTC, NOAA-9), and the third (c) shows a storm over northeastern Spain on 21 July 1989 (1535 UTC, NOAA-9). All gray-scale images shown cover an area approximately 260 × 340 km.

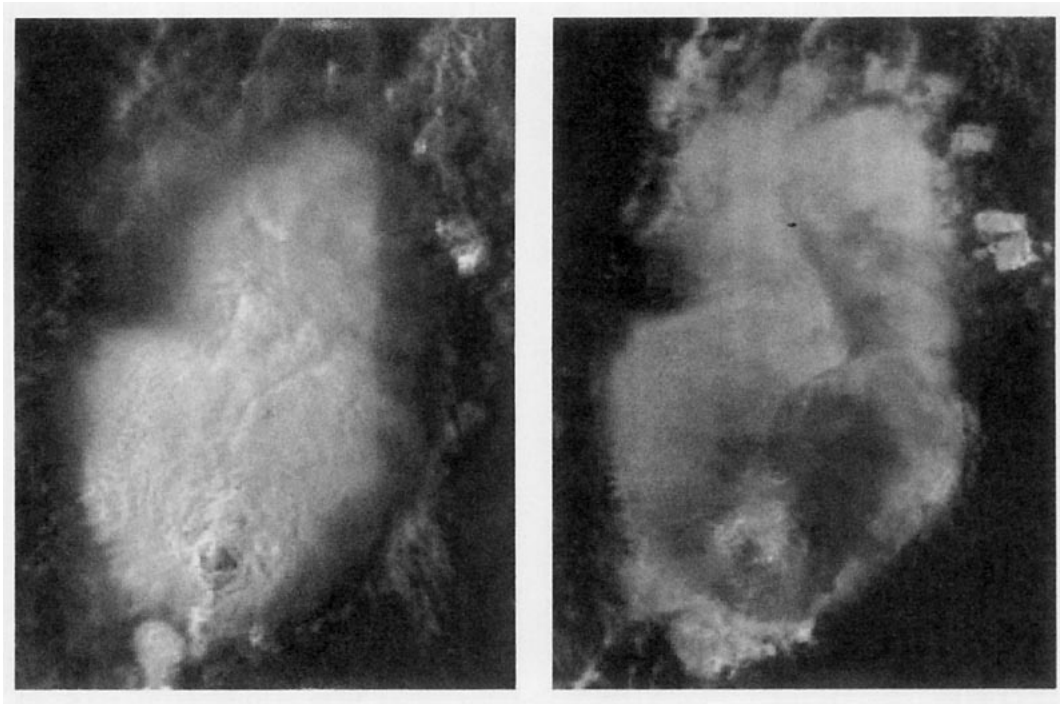

FIG. 1. (*Continued*)

The value of N_3 is obtained from the calibration relation between counts and radiances for each pixel, while $S_3(r, \xi)$ is calculated from (3) if the actual values of r and ξ are known.

Some simplification is necessary in practice, in order to determine the value of $N_3(T)$. To determine the temperature T, one can use the channel 4 (10.3–11.3 μm) data provided $\epsilon_4 = 1$ (i.e., a blackbody). Since real values of ϵ_4 are always less than one, this is a source of error in the computations. However, for sufficiently deep clouds, setting ϵ_4 to unity is a reasonable approximation (see Stephens 1978).

In summary, the technique employs the following simplifications.

(i) Absorption and dispersion of the incident, reflected, and emitted radiation are neglected.

(ii) Deviations from unit emissivity are neglected when determining the temperature T from the channel 4 radiances.

(iii) The effect of water vapor on channel 4 data is neglected.

(iv) Zero transmissivity is assumed.

(v) Diffuse reflection (Lambertian surface) is assumed.

3. Convective storms as observed by channel 3

Assuming the cloud tops of the convective storms are composed of ice particles only (i.e., no liquid water present), the infrared (IR) channels should depict them as a blackbody (Scorer 1987). Thus, their CH3 CTR should be very near zero; they should be reflecting very little of the incident solar radiation within the channel 3 window. Since the temperatures of deep convective cloud tops are relatively low (around −60°C), the amount of emitted radiation in this channel should also be low, so deep convective cloud tops should show very low total radiances in channel 3 imagery.

Gray-scale channel 3 images will be exhibited with an enhancement curve where higher radiances are depicted as darker in comparison with lower radiances. Therefore, ice-dominated convective cloud tops should appear nearly white. Although this is true for most of the observed convective storms, from time to time a storm is seen with either part of or virtually all of its top darker than surrounding storms (i.e., enhanced channel 3 radiance—see also Liljas 1987). By examining the channel 4 images, it should be possible to tell whether or not the enhanced radiance in the channel 3 images is attributable to emitted radiation. If it turns out that this is not the case, then (4) indicates the source for the high radiance must be sought in enhanced CH3 CTR.

Since the NOAA satellite is a polar orbiter, it passes over the convection at a more or less fixed time each day, a time which varies from one spacecraft to another. Unlike observations from geostationary satellites, there is no opportunity to observe the evolution of features during convective storm life cycles. Thus, some of the variation seen in the channel 3 radiances may be due to differences in the stage of development of the convection at the time the images are made. The signatures shown seem to appear in virtually all stages of development, however. As shown, there are at least two different signature categories associated with storms having enhanced CH3 CTR (see also Setvak 1989).

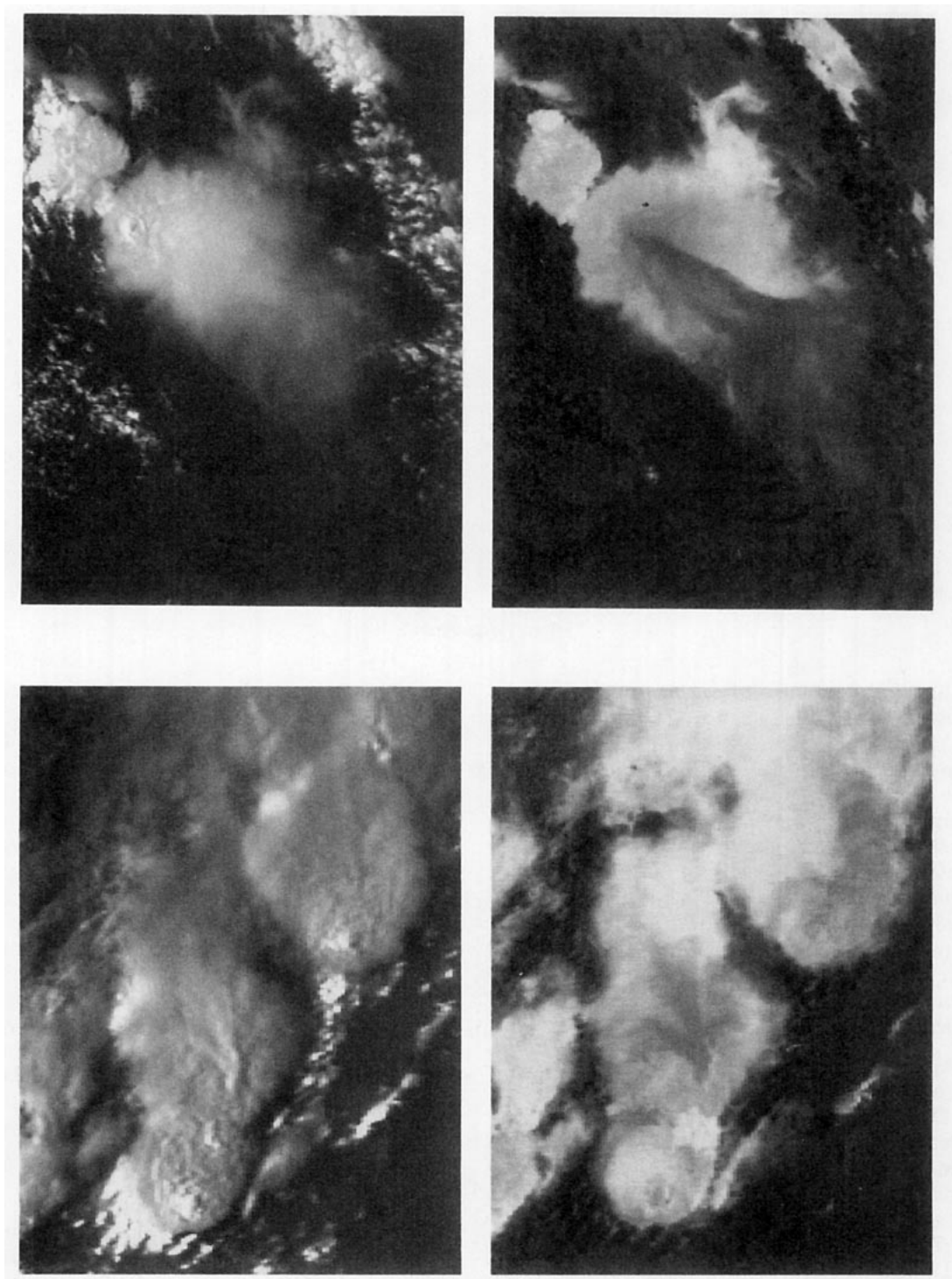

FIG. 2. Examples of storms exhibiting "plume-like" signatures, as in Fig. 1. The first example (a) shows storms over Rumania on 14 June 1987 (1320 UTC, NOAA-9), while the second is a storm over southeastern Poland on 18 August 1989 (1520 UTC, NOAA-9).

The first signature is called the *convective cell* type. Examples of this are shown in Fig. 1. In Fig. 1a, the enhanced reflectivity seems to be spread over the entire top of the convective cell, whereas in Fig. 1b the increased reflectivity seems to be localized near an overshooting cumulonimbus tower. Figure 1c appears to depict a case where a new overshooting tower has terminated the production of the enhanced reflectivity.

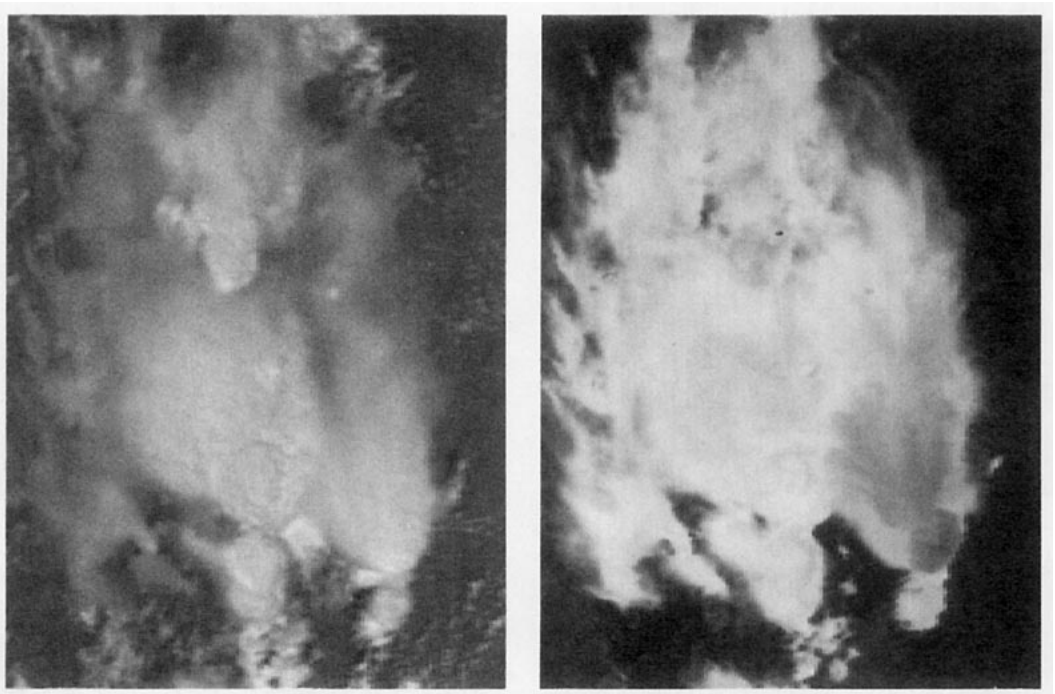

FIG. 3. Storms (as in Fig. 1) over southern Germany on 8 July 1989 (1315 UTC NOAA-11), showing an example of a storm (on the right) that exhibits both "convective cell" and "plume-like" signatures at the same time.

The second signature type is called *plume-like* for reasons that are obvious in Fig. 2. As shown in Fig. 2a, the source of enhanced CH3 CTR is coming from an apparent point source (recall that the size of a single pixel in the image is about 1 km). In the center of Fig. 2b, there is a plume that seems to divide into two streams. Note the convective cell-type signature with the storm in the upper-right part of the figure at the same time.

The two mechanisms for production of enhanced CH3 CTR seem to be independent, as shown in Fig. 3, that depicts a storm that displays both signatures at the same time. To date, this is the only example of a storm producing both signatures simultaneously. Generally speaking, it appears from the limited sample seen so far that the convective cell-type signature is the most common.

Convective storms sampled so far reveal a maximum value [as determined from (7)] for CH3 CTR of about 12%, whereas ordinary storms exhibit values in the range from 1%–3%. When looking at the reflectivity of cold cumulonimbus cloud tops, it should be noted that the proposed method for determining the reflectivity is only minimally contaminated by thermal emission. Thus, it seems plausible to suggest that an explanation for the observed signatures is related in some way to the microphysical properties of the cloud; namely, the size, shape, and phase of particles present. Thus, CH3 CTR can be viewed as a source of information about the microphysical processes operating within the cumulonimbus.

Of considerable interest is the suggestion of a connection between increased CH3 CTR and the occurrence of hail at the surface. This work has focused on storms in Europe, where the reporting of severe weather is even more sporadic than in the United States (see Kelly et al. 1985 for a discussion of reporting of nontornadic severe storm events in the United States). Nevertheless, even with this limited reporting, whenever a significant hailstorm was reported and AVHRR channel 3 data were available (e.g., as in Fig. 4), the hail event was associated with storms having such signatures. In Fig. 4b, the coldest cloud is in the form of a U-shaped region near the edge of the anvil, with a warm spot inside the "U" as described by McCann (1983). Such structures (often having a V-shape rather than the U-shape shown here) have been shown by Adler et al. (1985) to be related to thunderstorm intensity. However, both Adler et al. and McCann indicate that many severe storms do not have this feature. Note that Adler and Mack (1986) have concluded that a completely satisfactory explanation for these features in thunderstorm anvils is not yet available.

To date, a similar effort to tie hail (and/or any other severe weather) occurrence to enhanced CH3 CTR signatures using the somewhat more reliable severe weather reporting data in the United States remains undone. To our knowledge, this study is the first even to note the possibility of such a connection. Only a few of the storms showing enhanced CH3 CTR signatures also exhibit V- or U-shaped cold top structures with warm wakes in their concurrent channel 4 images.

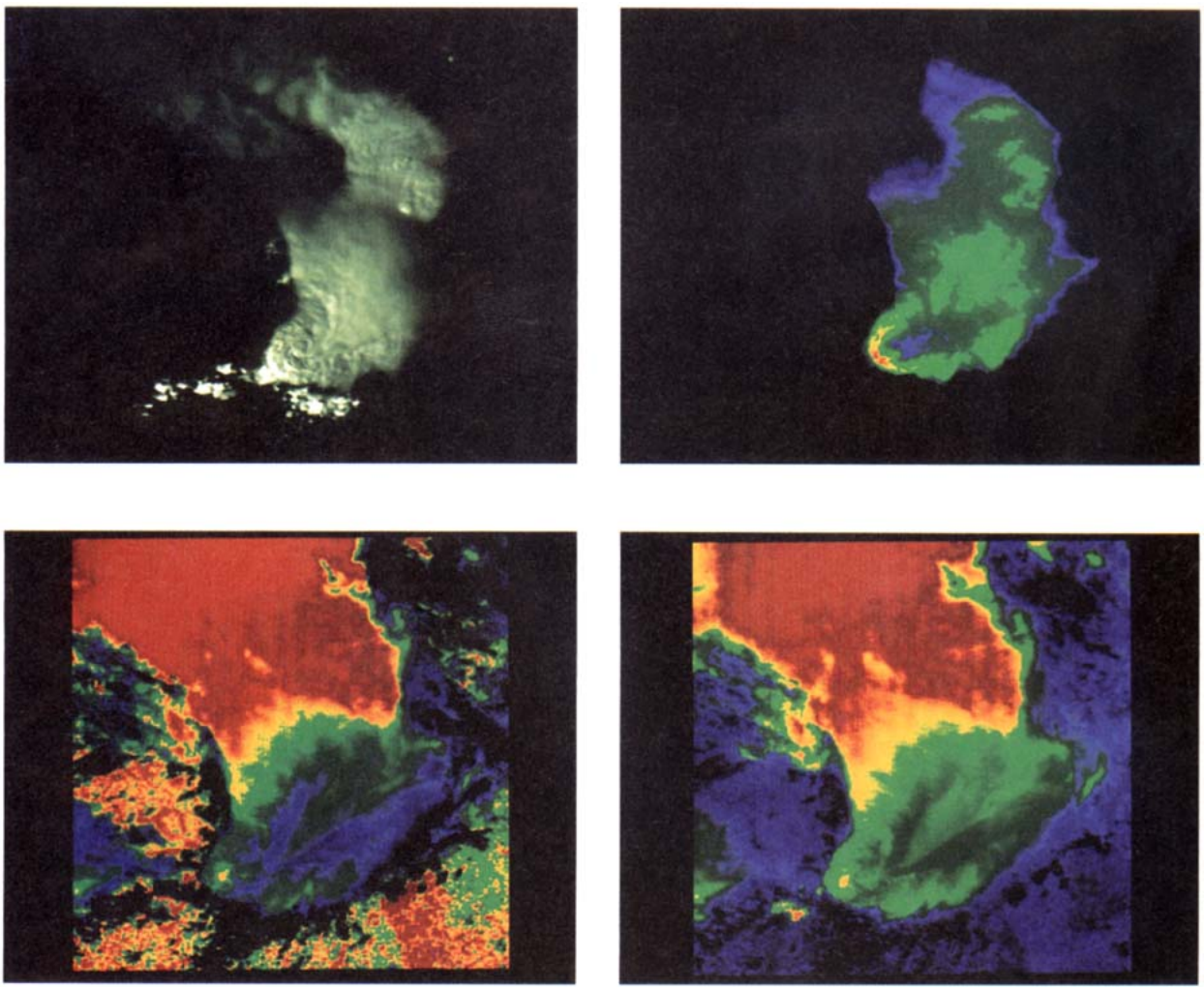

FIG. 4. Several images of a severe storm over Czechoslovakia on 18 August 1986 (1330 UTC, NOAA-9), which produced reported hailstones 12 cm in diameter. The area shown is approximately 250 × 250 km. The visible image is in (a), while an enhanced IR image is seen in (b), with a range of temperatures from −40° (dark blue) to −72°C (dark red). The original channel 3 image is seen in (c), with the lowest radiances shown in red, while green and blue correspond to higher radiances. Finally, (d) is a result of the image processing described in the text to reveal reflectivity. Areas with $\alpha \leq 3\%$ are shown in red and those with channel 3 reflectivity from 7% to 10% are in blue. The black around the storm indicates lower clouds composed of water droplets with channel 3 reflectivity higher than the range shown in the image. A cloud top outflow from the center of the storm is shown clearly—note that the source of the plume is downstream of the "cold V" and near the "warm wake" features (Heymsfield and Blackmer 1988) in the channel 4 image.

Moreover, not all the storms with the channel 4 signatures reveal enhanced CH3 CTR signatures. For the case shown in Fig. 4, the "source point" for the plume appears to be near the warm spot inside the U-shaped feature (compare Fig. 4d with Fig. 4b) in the channel 4 images. If it turns out that an association between the enhanced CH3 CTR signatures and severe weather can be validated, it could increase the capability to use satellite images to detect severe storms, since the "enhanced-V/warm spot" signature has a relatively low detection rate (Adler et al. 1985).

4. Discussion

While we do not pretend to have a satisfactory explanation for the observed signatures, there are some ideas that are offered as speculation. It may be that storms with very strong updrafts produce supercooled water drops, even at the very cold temperatures associated with deep convective storm tops. We admit this seems quite unlikely at the −60°C temperatures typical of cumulonimbus anvils. To date, the primarily European observations are not backed up with concurrent

radar-measured cloud top heights, soundings, and so forth. Therefore, we are not yet able to give a complete specification of the environmental variables for most of the observed events.

Perhaps the most vigorous updrafts tend to produce large amounts of very small ice particles (sizes on the order of 2–4 μm, which are near the channel 3 spectral range), thereby enhancing reflectivity. Arking and Childs (1985) have provided a detailed look at the theoretical sensitivity of channel 3 reflectance to particle size and phase (see their Fig. 1); the results indicate high reflectance for particles near the wavelength of the channel 3 nominal wavelength. While they do not discuss it, for even smaller particles, the reflectance must decrease as one goes into Rayleigh scattering.

Many of the storms that show either the "convective cell" or "plume-like" signatures do not have any other known signatures in the available satellite imagery. If, as McCann (1983) has speculated, the enhanced-V/warm spot signature is associated with supercells, then there are many severe storms that will not be detected using that signature, since only a fraction of severe storms are supercells. While a quantitative, statistical relationship between enhanced CH3 CTR signatures and severe weather has not been established, the possibility seems to warrant some additional exploration.

This could be done using the historical archives of AVHRR data and the reports of severe weather. It also could be done in near real time by examining the AVHRR images on severe weather days. It is noteworthy, however, that present plans for the NOAA satellite call for shutting down channel 3 during daylight hours in 1992. While the geostationary satellites have a channel that is comparable to the AVHRR channel 3, the resolution is sufficiently coarse ($\sim$40 km vs $\sim$1 km in the NOAA spacecraft) that the features pointed out would not be resolved, in general. It appears that the next generation of geostationary satellites will provide reasonably good spatial resolution in the range of 3.7 μm with the added advantage of being able to monitor the time evolution of these signatures.

The main purpose in this note has been to stimulate interest in the channel 3 data stream. If the apparent connection between the CH3 CTR signatures and severe weather can be given a reasonable validation, and if the signatures can be detected prior to the occurrence of severe weather at the surface, then applications for the channel 3 data in severe weather forecasting/nowcasting virtually are guaranteed. Should it turn out that the signatures are well correlated with severe weather but there is little or no lead time, then at the very least we have a way of increasing the chances of detecting the presence of severe weather in remote areas for climatological purposes.

Acknowledgments. The authors wish to thank Drs. R. Maddox and R. Rabin of NSSL for their valuable comments on an early version of the manuscript. The junior author also would like to thank the WMO for its sponsorship of the interaction trip to Czechoslovakia that produced this paper.

REFERENCES

Adler, R. F., and R. A. Mack, 1986: Thunderstorm cloud top dynamics as inferred from satellite observations and a cloud top parcel model. *J. Atmos. Sci.*, **43**, 1945–1960.

——, M. J. Markus and D. D. Fenn, 1985: Detection of severe Midwest thunderstorms using geosynchronous satellite data. *Mon. Wea. Rev.*, **113**, 769–781.

Arking, A., and J. Childs, 1985: Retrieval of cloud cover parameters from satellite images. *J. Climate Appl. Meteor.*, **24**, 322–333.

d'Entremont, R. P., and T. J. Kleespies, 1988: Possible measurement errors in calibrated AVHRR data. Air Force Geophysics Laboratory Tech. Rept. 88-0105, Environmental Research Paper No. 1001, Hanscom Air Force Base, 21 pp.

Heymsfield, G. M., and R. H. Blackmer, Jr., 1988: Satellite-observed characteristics of Midwest severe thunderstorm anvils. *Mon. Wea. Rev.*, **116**, 2200–2224.

Kelly, D. L., J. T. Schaefer and C. A. Doswell III, 1985: Climatology of nontornadic severe thunderstorm events in the United States. *Mon. Wea. Rev.*, **113**, 1997–2014.

Lauritson, L., G. J. Nelson and F. W. Porto, 1979: Data extraction and calibration of TIROS-N/NOAA radiometers. NOAA Tech. Memo. NESS 107, NESDIS, World Weather Building, Camp Springs, 73 pp.

Liljas, E., 1987: Multispectral methods for cloud classification. *Proc., Satellite and Radar Imagery Interpretation Workshop,* Reading, England, European Organization for the Exploitation of Meteorological Satellites, 475–493.

McCann, D. W., 1983: The enhanced V, a satellite observable severe storm signature. *Mon. Wea. Rev.*, **111**, 887–894.

Setvák, M., 1989: Convective storms—the AVHRR channel 3 cloud top reflectivity as a consequence of internal processes. *Proc., Conference on Weather Modification and Applied Cloud Physis,* Beijing, World Meteor. Org., 109–112.

Scorer, R. S., 1987: Convective rain as seen by channel 3. *Proc., Satellite and Radar Imagery Interpretation Workshop,* Reading, England, European Organization for the Exploitation of Meteorological Satellites, 509–513.

Stephens, G. L., 1978: Radiation profiles in extended water clouds. Part II: Parameterization schemes. *J. Atmos. Sci.*, **35**, 2123–2132.